Article

Delivery of dCas9 Activator System Using Magnetic Nanoparticles Technology as a Vector Delivery Method for Human Skin Fibroblast

Mahdi Mohammadi Ghanbarlou [1,2], Shahriyar Abdoli [1,3], Hamed Omid [1], Leila Qazizadeh [1], Hadi Bamehr [1], Mozhgan Raigani [4], Hosein Shahsavarani [5,2], Morteza Karimipour [4] and Mohammad Ali Shokrgozar [1,2,*]

1   National Cell Bank of Iran, Pasteur Institute of Iran, Tehran 1316943551, Iran
2   Laboratory of Regenerative Medicine and Biomedical Innovations, Pasteur Institute of Iran, Tehran 1316943551, Iran
3   Biotechnology Research Center, Golestan University of Medical Sciences, Golestan 1575949138, Iran
4   Biotechnology Research Center, Pasteur Institute of Iran, Tehran 1316943551, Iran
5   Department of Cell and Mol Biology, Shahid Beheshti University, Tehran 1983969411, Iran
*   Correspondence: mashokrgozar@pasteur.ac.ir

Abstract: The overexpression of stem cell-related genes such as octamer-binding transcription factor 4 (OCT4) and (sex determining region Y)-box 2 (SOX2) has been indicated to play several critical roles in stem cell self-renewal; moreover, the elevation of the self-renewal of cancer cells with stem cell-like properties has been suggested. The clustered and regularly interspaced short palindromic repeats-associated protein 9 (CRISPR/Cas9) protein fused to transactivation domains can be used to activate gene expression in human cells. CRISPR-mediated activation (CRISPRa) systems represent an effective genome editing tool for highly specific gene activation in which a nuclease-deficient Cas9 (dCas9) is utilized to target a transcriptional activator to the gene's regulatory element, such as a promoter and enhancer. The main drawback of typical delivery methods for CRISPR/Cas9 components is their low transfection efficiency or toxic effects on cells; thus, we generated superparamagnetic iron oxide nanoparticles (SPIONs) coated with polyethylenimine (PEI) to improve the delivery of CRISPR/Cas9 constructs into human foreskin fibroblast cells. The delivery system with magnetic PEI-coated nanoparticles complex was applied to constitute plasmid DNA lipoplexes. CRISPRa systems were used to overexpress the endogenous OCT4 and SOX2 in fibroblast cells. The quantitative polymerase chain reaction (QPCR) assessment exhibited a three-times higher expression of OCT4 and SOX2 transfected by CRISPRa using MNPs. Moreover, no additional cytotoxicity was observed with the application of magnetic nanoparticles (MNPs) compared to lipofectamine. Our results demonstrate that MNPs enable the effective delivery of the CRISPR/Cas9 construct into human foreskin fibroblasts with low cell toxicity and a consequential overexpression of endogenous OCT4 and SOX2.

Keywords: CRISPR/dcas9 activator system; human skin fibroblast; OCT4; SOX2; superparamagnetic iron oxide nanoparticles (SPIONs)

1. Introduction

Gene expression is tightly controlled in the biological processes, including development, differentiation, and proliferation. Pluripotent stem cells showed great promise for regenerative medicine. The capability of directly regulating endogenous pluripotent gene expression without delivering the exogenous factors facilitates the study of the mechanism under human disease [1]. In this context, reprogramming differentiated somatic cells into induced pluripotent stem cells (iPSCs) can be performed through the ectopic expression of OCT4, SOX2, KLF4, and c-Myc (OSKM) [2]. The overexpression of OCT4, SOX2, and KLF4 initially targets to remodel endogenous loci through the genome, consequently makes pluripotent regulatory circuitry [3].

Recently, the use of CRISPR/Cas9 technology as a new tool for genomics engineering has attracted much attention due to its potential in biotechnological applications [4,5]. Generally, the CRISPR system consists of a single CRISPR-associated Cas9 protein and small guide RNAs (gRNAs); the components of the CRISPR/Cas9 system can be introduced into cells in three forms: as a plasmid, as mRNA, or as a ribonucleotide protein (RNP) [5,6]. Regarding CRISPRa, dCas9 can be used to activate gene expression through the direct targeting of endogenous loci [7].

The efficient delivery of single-guide RNA (sgRNA) and the enzyme Cas9 is a promising therapeutic strategy for successful cell modification [8]. In this context, two kinds of gene caries including viral and non-viral vectors are presented [8]. Despite the excellent transfection efficacy of viral vectors, the main drawbacks of applying viral vectors in clinics are their limited DNA packing cargo size and safety issues [9].

However, non-viral delivery systems such as physical (electroporation or nucleofection) and chemical (lipofection or polyfection) delivery systems have the potential to transfer larger gene sequences [10]. Moreover, some strategies such as magnetofection can supply an external stimulus to assist vectors to increase gene expression. Magnetofection is represented as an ideal method for rapid and highly efficient transfection [11]. In addition, magnetofection based on superparamagnetic iron oxide nanoparticle (SPION)-carrying plasmid DNA can improve the accumulation of nucleic acids in a specific area with an external magnetic field, which results in an increase of several hundred folds in gene expression [12]. A previous study has demonstrated the potential of cationic magnetic particles including polyethylenimine (PEI) [13]-coated SPION as efficient magnetoplexes for plasmid DNA delivery [14]. The cationic polymers-coated SPION showed a reduction in cytotoxicity compared to the cationic polymers themselves [15]. A study has indicated that the transfection efficiency of the magnetoplex is improved when an external magnet is placed nearby; thus, a higher expression of miRNA-123 is displayed when using the CPIO/pMIRNA-128 gene delivery system [15].

The application of MNPs to the delivery of the CRISPR/Cas9 construct into porcine fibroblast cells under the influence of an external magnetic field has displayed an improved transfection efficacy [16]. CRISPRa-mediated POU5F1 (OCT4) activation has been used to replace transgenic OCT4 in human fibroblast reprogramming. However, transgenic expression of only OCT4 has been shown to be sufficient for the reprogramming of neuroepithelial stem cells (NSCs) into iPSCs [5,17].

In this study, we test the potential of SPIONs coated with PEI to enhance the delivery of CRISPR/Cas9 constructs into human foreskin fibroblast cells and the consequent overexpression of endogenous OCT4 and SOX2.

2. Materials and Methods

2.1. Guide RNA Design and dCas9 Activator Plasmid

The dCas9 expression vector, pCXLE-dCas9VP192-T2A-GFP-shP53, was kindly gifted from Timo Otonkoski, Centre of Excellence in Stem Cell Metabolism Helsinki One Health (HOH). The sgRNAs were designed using the ChopChop tool (https://chopchop.rc.fas.harvard.edu/) (accessed on 16 September 2021) according to the algorithm used by this program. The sgRNAs were designed to target the proximal promoter regions of OCT4 and SOX2 (Table 1).

Table 1. sgRNA target sequence on human OCT4 and SOX2 promoters.

sgRNA Name	Target Sequence (5′-3′)
OCT4 (1)	GGGGGAGAAACTGAGGCGA
OCT4 (2)	GACACAACTGGCGCCCCTCC
SOX2 (1)	TCTGTGGGGGACCTGCACTG
SOX2 (2)	GGCACAGTGCCAGAGGTCTG

2.2. Synthesis of SPIONs

Fe$_3$O$_4$ MNPs were generated using a co-precipitation method as described by Tiwari et al. in 2016 [18]. Briefly, FeCl$_3$·6H$_2$O (1.0 mmol) and FeSO$_4$·7H$_2$O (2.0 mmol) were mixed in

100 mL of deionized water, heated to 80 °C, and then the NaOH solution (1.0 M) was slowly added to the mixture until the pH reached up to 11, with shaking allowing them to be precipitated. Fe_3O_4 NPs were formed when the precipitate color turned black from their original light brown. Then, the black mixture was stirred for 15 min and underwent hydrothermal treatment by transferring it to a sealed autoclave for 30 min at 70 °C, and the reaction mixture was cooled down to room temperature. The SPIONs were separated via magnetic separation and the sample impurities were removed by washing with deionized water. Finally, the SPION was suspended in the deionized water for further use.

2.3. Synthesis of PEI-Coated MNPs Complexed with CRISPR-Cas9 Plasmid

PEI-coated MNPs were prepared at (N/P) conjugation ratio of 10/1 (nitrogen in PEI-coated MNPs/phosphorus in DNA), which was performed by mixing volumes of the aqueous solution of PEI, DNA, and MNPs, as reported by Zhang et al. [19,20]. Briefly, magnetic complexes were prepared by mixing 50 µL of PEI (40 µg/mL) and 2 µg of plasmid DNA, and the mixture was incubated with MNPs for 20 min at room temperature [20].

2.4. Physicochemical Characterization

Physicochemical characterization including the size distribution and zeta potential of CRISPR/Cas9-PEI–SPION was conducted using the DLS device (Sympatec, NANOPHOX Model, Clausthal-Zellerfeld, Germany) based on the number of particles. Samples were sonicated for 1–2 min in injectable distilled water. He–Ne laser beam measurements were conducted by detecting at a scattering angle of 90° at 633 nm at 25 °C.

The zeta potential was measured using a universal zeta dip cell. The morphology and the particle size of the MNPs were determined using field emission scanning electron microscopy (FESEM). The magnetic properties of the synthesized Fe_3O_4 were evaluated using a vibrating sampling magnetometer (VSM) at room temperature.

2.5. Isolation and Primary Culture of Dermal Fibroblasts

Before starting, all tools, including surgical sets, culture vessels, PBS, etc., were sterilized via autoclaving at 121 °C and high pressure. The work environment was also sterilized using alcohol 70% and ultraviolet radiation. The steps taken for the isolation and primary culture of the dermal fibroblasts were as follows: First, neonatal foreskin was beheaded using sterile tools, and then small pieces of their skin was removed with forceps and transferred to petri dishes containing Dulbecco's Phosphate Buffered Saline (dPBS) on ice. Neonatal foreskin pieces were split into smaller pieces using a scalpel and transferred to 15-mm Falcon tubes along with the dPBS. They were moved up and down for washing and crushing. For particles deposited after centrifuge at 1000 rpm for 2 min, dPBS was removed from the Falcon tube, and trypsin 0.1% was added to the cells. The tubes were placed in a shaking incubator at 37 °C for 10 min and then centrifuged at 1100 rpm for 2 min, and trypsin was removed from the tubes. A culture medium containing FBS 10% was used to neutralize trypsin. That is, an amount of the medium equal to trypsin volume was added to the Falcon tubes, and, after moving up and down, they were then centrifuged at 1100 rpm for 2 min. Then, the medium containing trypsin was removed from the tubes and once again added to the cells, and the cells were transferred to culture flasks containing the culture medium. Culture flasks were incubated at 37 °C and 5% CO_2 and 95% humidity. The medium was changed 72 h after primary culture. The morphology of the cells was assessed at all stages using a fluorescent microscope (Olympus).

2.6. Cell Culture

Human foreskin fibroblast cells were isolated from healthy neonatal donors (age, ~6 months) at Shariati Hospital, Tehran, Iran. HEK 293 was obtained from the National Cell Bank of Iran (Pasteur Institute, Tehran, Iran). These cell lines were cultured in Dulbecco's modified Eagle's medium (DMEM; Life Technologies, Grand Island, NY, USA) supplemented with 10% fetal bovine serum (FBS; Gibco, Grand Island, NY, USA), 2 mM

GlutaMAX (Life Technologies, Grand Island, NY, USA), and 100 μg/mL penicillin/streptomycin (Life Technologies, Grand Island, NY, USA), and incubated at 37 °C with 5% CO_2 incubation. Forty-eight hours prior to transfection, the cells were seeded in 12-well plates at a density of 2×10^5 cells/well in 1 mL of culture medium (TPP, Sigma Aldrich, Munich, Germany).

Plates were incubated at 37 °C when the cell confluency reached up to ~60–70% at the time of transfection. Cells in the absence of CRISPR/Cas9-PEI-MNP cells were transfected with lipofectamine 3000 (Thermo Fisher Scientific, Waltham, MA, USA), using the standard protocol as control.

2.7. Magnetofection

For magnetofection, the CRISPR/Cas9-PEI-MNPs (2 μg DNA/well) were incubated with cultured cells in serum-free media for 2 min. The plate was placed on a sintered Mega Magnetic Plate and incubated for 20 min (37 °C, 5% CO_2) to help the complex spin the cells' surface. This step is followed by a 24 h incubation period with a fresh media in the absence of a magnetic field at 37 °C, in a 5% CO_2 humidified atmosphere. Finally, the cells were washed 2 times with PBS, trypsinized, and then resuspended in 800 μL media to obtain a final volume of 1 mL.

2.8. Evaluation of Transfection Efficiency by Fluorescent Microscopy

Following transfection, plates were incubated for 24 h with these magnetic complexes. Cell growth and morphology were assessed for control, lipofection, and magnetofection groups using fluorescence microscopy.

2.9. Flow Cytometer Analyses

Cells were trypsinized, washed three times with PBS solution to remove the bounded MNPs, and resuspended in fresh DMEM for further analysis using a flow cytometer. Positive green fluorescent protein (GFP)-expressing cells were analyzed using a flow cytometer instrument. The presented data were analyzed using FlowJo software V10. GFP fluorescence intensity was graphed using a dimensional dot plot of 488 nm excitation and emission was detected at 530/30 versus 575/30 nm or 530/30 versus 695/40 nm, respectively.

2.10. Real-Time RT-PCR (qRT-PCR)

HEK293T and HFF cells were seeded in a 6-well plate (SPL, Pyeongtaek, Republic of Korea) and transfected with either OCT4 or SOX2 plasmids using magnetofection technology we reported previously. Forty-eight hours later, the total RNA was isolated using the High Pure RNA isolation Kit (Roche, Mannheim, Germany). DNase treatment was performed to eliminate genomic DNA contamination using DNase I enzyme (Thermo Fisher Scientific Inc., Waltham, MA, USA). Total RNA concentration was measured using Nanodrop (NanoDrop Technologies Inc., Wilmington, DE, USA), and 1 μg of RNA was used to synthesize cDNA in a 40-μL reaction using the Biotechrabbit™ cDNA Synthesis Kit (Biotechrabbit, Berlin, Germany) according to the manufacturer's instructions. The real-time RT-PCR was carried out with the SYBER Green I Master mix (Roche Diagnostics, Ottweiler, Germany). Gene amplification was conducted with an ABI 7500 (ABI, Applied Biosystems, New York, NY, USA) in a 20 μL reaction. Thermal cycling conditions were applied as follows: initiation for 10 min at 95 °C, followed by 40 cycles of 15 s at 95 °C, 30 s at 60 °C, and 15 s at 72 °C.

The relative mRNA expression levels were calculated using the $\Delta\Delta$CT method, where glyceraldehyde-3-phosphate dehydrogenase (GAPDH) served as the endogenous control and un-transfected cells were the negative control. All of the PCR reactions were run in triplicate.

2.11. CRISPR-Mediated Activation of OCT4 and SOX2 Promoters in Human Foreskin Fibroblast

Human skin fibroblasts (HFFs) were detached as single cells from the culture plates with TrypLE Select (Gibco) and washed with PBS. Cells at a density of 10^6 were transfected with 6 μg of plasmid mixture, containing 2 μg of dCas9 activator plasmid

(pCXLE-dCas9VP192-GFP-shp53) and 4 µg of guide plasmids. Then, fibroblasts were plated on matrigel-coated cell culture plates in a fibroblast medium. After 4 days, the cell culture medium was changed to a 1:1 mixture of fibroblast medium and hES-medium (KnockOut DMEM (Gibco) supplemented with 20% KO serum replacement (Gibco), 1% GlutaMAX (Gibco), 0.1 mM beta-mercaptoethanol, 1% nonessential amino acids (Gibco), and 6 ng/mL basic fibroblast growth factor (FGF-2; Sigma)) supplemented with sodium butyrate (0.25 mM; Sigma). When the first colonies started to emerge, the cell culture medium was changed to the hES-medium until the colonies were picked.

2.12. Toxicity Assay

The cytotoxicity of the magnetic complexes was evaluated using an MTT cell toxicity assay. The cells were seeded at a density of 5×10^3 cells/well on a 96-well plate (TPP, Sigma Aldrich) in 100 µL of supplemented DMEM and incubated for 24 h until it reached a confluency of 70%. The cells were transfected with 20 pg of CRISPR/Cas9-PEI-MNPs using a Mega Magnetic Plate. Moreover, cells were transfected with lipofectamine and incubated for 24 h. Then, the supernatant was replaced with fresh DMEM, and 25 µL of a 5.5 mg/mL MTT reagent was added to the cells. The cells were incubated for 3 h in the dark, and, finally, the supernatant was removed, and the remaining purple formazan was lysed with 100 µL of DMSO for 40 min. The assay was performed in triplicate.

Absorbance was measured using an enzyme-linked immunosorbent assay (ELISA) reader (Bio Tek Instruments, Inc., Winooski, VT, USA) at 570 nm. The cell viability was calculated from the absorbance versus concentration curve.

2.13. Statistical Analysis

The experiments were performed in triplicate, and the results are expressed as means ± standard deviation. A paired t-test, one-way analysis of variance with Bonferroni's post hoc test, or a two-way analysis of variance with a post hoc test, were used for statistical analysis. The *p*-values of <0.05 were considered significant. Statistical analysis was performed using commercially available software IBM® SPSS® Statistics software (IBM Corp., Armonk, NY, USA).

3. Results

3.1. Synthesis of CRISPR/Cas9-PEI-MNPs Complex

The synthesis of the CRISPR/Cas9-PEI-MNPs complex is schematically illustrated in Figure 1. According to Figure 1, SPIONs were synthesized, coated with PEI, and complexed with the CRISPR/Cas9 plasmid.
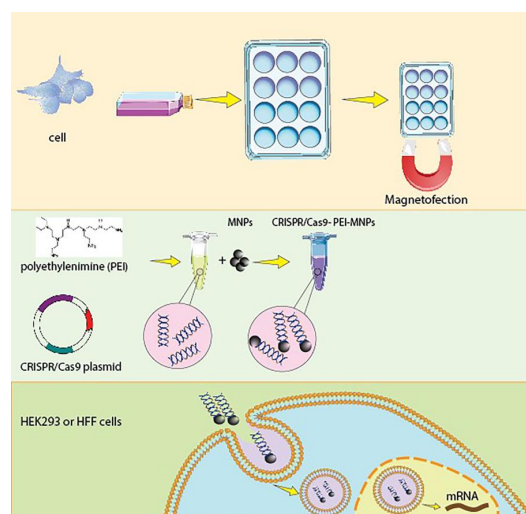

Figure 1. Schematic illustration of the synthesis of the CRISPR/Cas9-PEI-MNP complex. This system is constructed using the co-precipitation method, coated with PEI and further fused with a CRISPR/Cas9

plasmid to form a complex. The CRISPR/Cas9-PEI-MNP complex is transfected into HEK-293 and HFF cells via magnetofection. The CRISPR/Cas9-PEI-MNP complexes are internalized by the cells through the endocytosis pathway due to the cationic PEI.

3.2. Analysis of Physicochemical Properties and Stability of CRISPR/Cas9-PEI-MNPs' Complex

In order to evaluate the stability of the CRISPR/Cas9-PEI-MNP complex, physicochemical properties such as diameter and zeta potential were determined. The particle size of three formulations is shown in Figure 2A. The particle size of the MNPs was to be around 155 nm in diameter when in water. After the surface functionalization of MNPs using PEI, the particle size was slightly increased to 165 nm. In addition, the incorporation of CRISPR/Cas9 plasmid resulted in a significantly elevated particle size to around 1200 nm. In addition, when all three formulations were suspended in DMEM with 10% FBS, the average diameter of MNPs, PEI-MNPs, and CRISPR/Cas9-PEI-MNP particles were approximately 156 nm, 620 nm, and 158 nm, respectively.
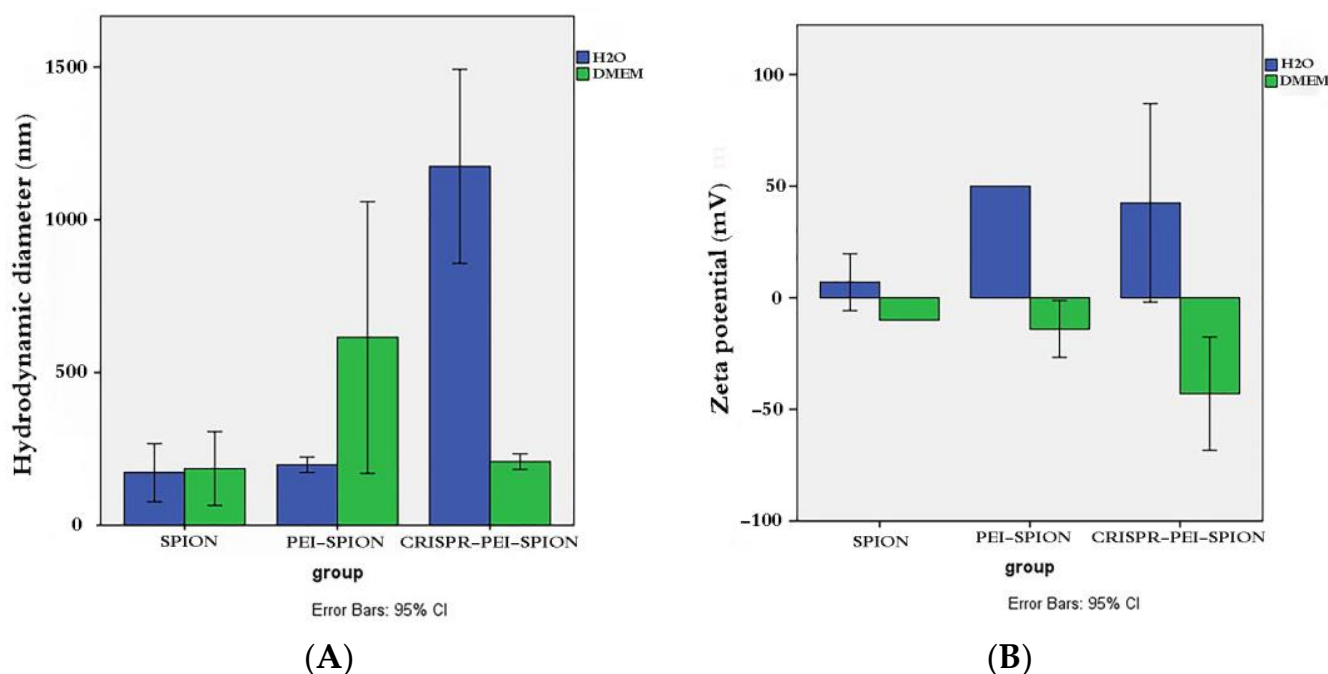

(A)   **(B)**

Figure 2. (**A**) Hydrodynamic diameter of magnetic nanoparticles (MNPs), PEI-MNPs, CRISPR/Cas9-PEI-MNPs in the presence of water and DMEM at pH 7.0 (mean ± S.D.; n = 3). (**B**) Zeta potential of magnetic nanoparticles (MNPs), PEI-MNPs, CRISPR/Cas9-PEI-MNPs in the presence of water and DMEM at pH 7.0 (mean ± S.D.; n = 3).

As indicated in Figure 2B, the zeta potential of MNPs, PEI-MNPs, and CRISPR/Cas9-PEI-MNPs at pH 7 possessed a positive charge in water (10, 50, and 49 mV, respectively). Moreover, the values of the zeta potential of the three MNPs became negative when the MNPs were suspended in 10% DMEM containing FBS (−10, −19.9, and −49.5 mV for MNPs, PEI-MNPs, and CRISPR/Cas9-PEI-MNPs, respectively).

3.3. Scanning Electron Microscopy

FESEM revealed that the MNPs fabricated using co-precipitation and the nanoparticles were homogeneous (Figure 3A). Moreover, the result of DLS showed that the MNPs possess superparamagnetic behavior as indicated in Figure 3B by measuring the magnetization curve of Fe_3O_4 nanoparticles.
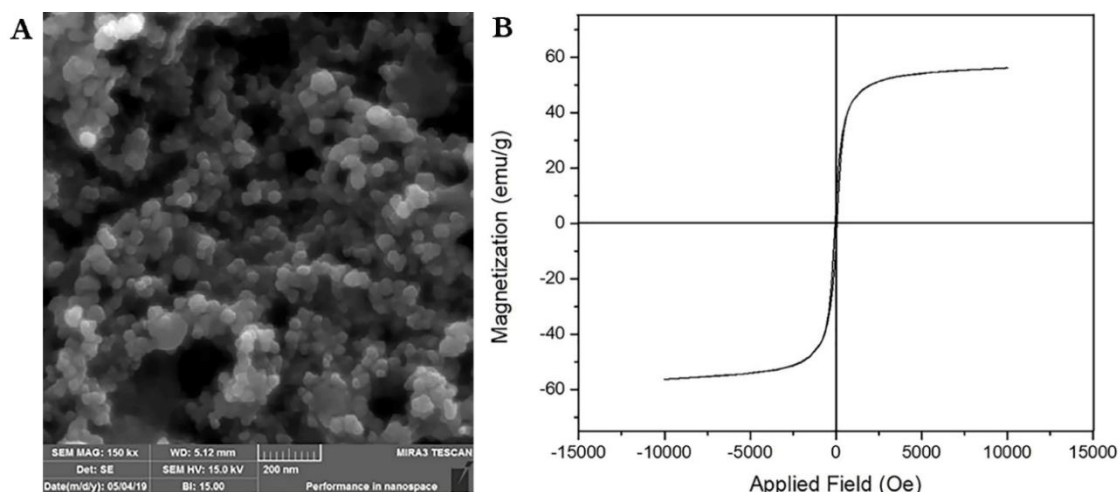
Figure 3. Ultrastructure of MNPs complex: (**A**) FESEM micrographs of magnetic-nucleic acid complexes. (**B**) Magnetization curve of MNPs.

3.4. Result of HFF Isolation

Fibroblasts cultured on different days were examined in terms of growth and morphology using a fluorescent microscope (Olympus) with 10× and 40× magnification. Figure 4 shows the morphology of fibroblasts from the first passage at different days. Finally, cells with a clear and oval to spindle-shaped stained nucleus, 1–2 nucleoli, and branched cytoplasm were observed to be consistent with the morphology of fibroblasts. The culture medium appeared clear without any turbidity or bacterial or fungal contamination.
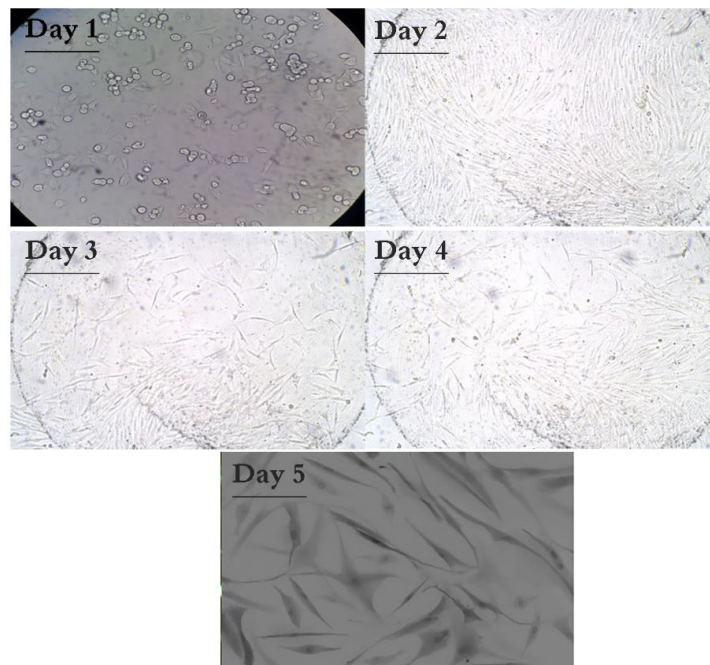
Figure 4. The morphology of fibroblasts from the first passage at different days (×40 magnification for days 1 to 4 and ×100 magnification for day 5).

3.5. Effect of Magnetic Field on Cellular Uptake and GFP Expression

Magnetic-based transfection has drawn considerable attention due to the accelerated cell surface assembling of magnetoplexes in the presence of a magnetic field and the consequent increase in gene expression. To investigate the effect of applying a magnetic field, we performed the transfection experiments with and without the influence of a

magnetic field. We also transfected using lipofectamine and measured the intensity of GFP expression. In the HEK-293 and HFF cells transfected using the CRISPR/Cas9-PEI-MNP complex, the fluorescent intensity was around 7.89% using lipofectamine, while this value increased up to 28.2% when magnetofection was used for the CRISPR/Cas9-PEI-MNPs' transfection of human foreskin fibroblasts (Figure 5A,B). Magnetofection could deliver the gene of interest (plasmid) better than lipofectamine 3000. Although there was no significant difference between the magnetofection and lipofection of HEK293 cells, the presence of a magnetic field might result in a significantly higher transfection efficiency of HFF cells, indicating that magnetic properties assist concentrations of magnetoplexes on the cell surface. Moreover, the microscopic observations were consistent with the transfection efficacy data obtained from flow cytometry experiments (Figure 5C). In HFF cells, the expression of GFP after the lipofection of the CRISPR/Cas9-PEI-MNP complex was observed to be around 7.89, while the magnetofection of this complex showed a transfection efficiency of 28.2 (Figure 5B).
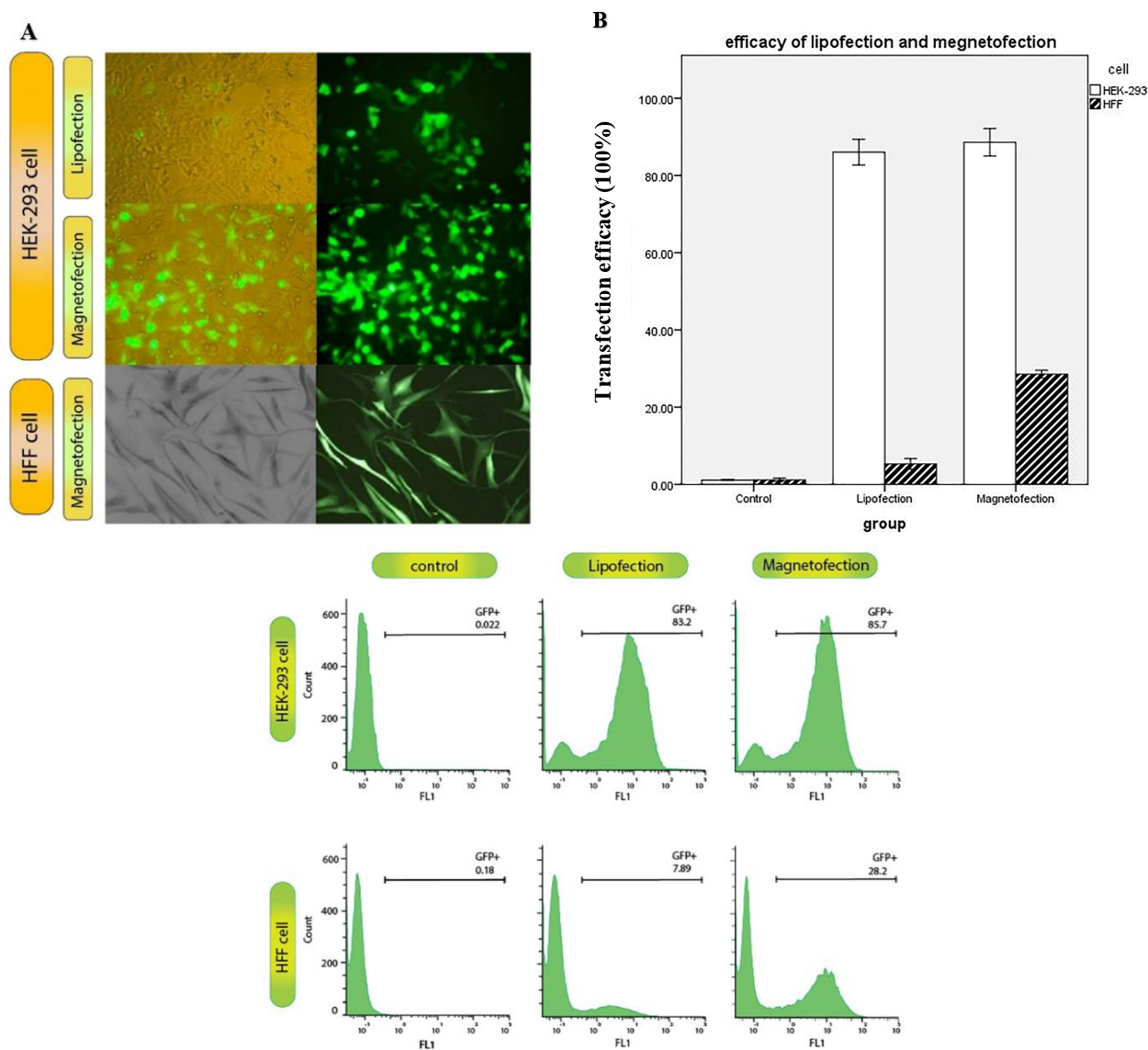

Figure 5. (**A**) Quantification of the transfection efficacy of the CRISPR/Cas9-PEI-MNP complex in the HEK-293 and HFF cells using two reagents. (**B**) Fluorescent microscopy image of the HEK293 and HFF cells transfected using the CRISPR/Cas9-PEI-MNP complex (×40 magnification for HEK-293 and ×100 magnification for HFF cell). (**C**) Flow cytometry representative data of the HEK-293 and HFF cells transfected using the CRISPR/Cas9-PEI-MNP complex.

3.6. Cytotoxicity

Although following the magnetofection of the CRISPR/Cas9-PEI-MNP complex, the viability of HEK-293 and HFF cells was lower in comparison with lipofection (76% vs. 82.0%, respectively), and MNPs showed biocompatibility with HEK-293 and HFF cells. Thus, as shown in Figure 6, the transfection with the MNPs did not reveal any significant cytotoxicity compared to the lipofectamine method ($p = 0.12$).
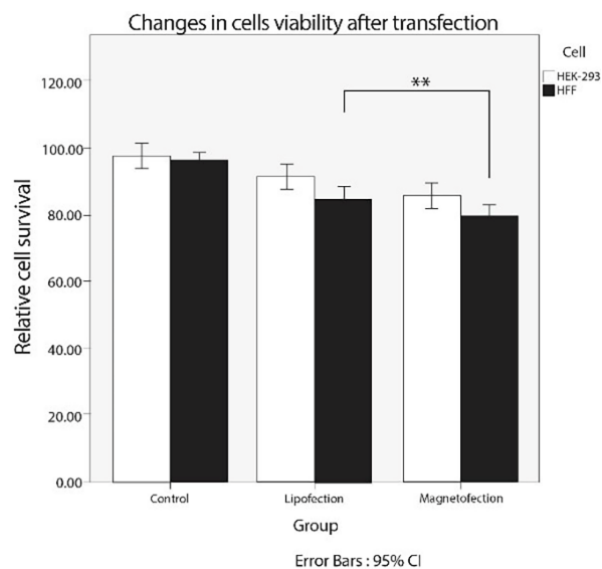

Figure 6. Assessment of cytotoxicity and cell viability using MTT assay 24 h post-incubation against CRISPR/Cas9-PEI-MNP complex-transfected HEK-293 and HFF cells using magnetofection and lipofectamine. The asterisks indicate a significant difference (** $p < 0.01$).

3.7. Activation of Endogenous OCT4 and SOX2

To generate the CRISPR activation for the OCT4 and SOX2 promoters, we designed sgRNAs which target the human endogenous OCT4 and SOX2 and tested in HFF and HEK-293 cells. Four sgRNAs were designed to span the promoters of OCT4 and SOX2. To test whether the magnetofection of pCXLE-dCas9VP192-T2A-GFP-shP53 with sgOCT4 and sgSOX2 can activate the OCT4 and SOX2 promoters in HFF cells, we co-transfected sgOCT4 and sgSOX2 with the pCXLE-dCas9VP192-T2A-GFP-shP53 plasmids. As a control, the HFF cells were magnetofected with only the pCXLE-dCas9VP192-T2A-GFP-shP53 plasmid. Two days after transfection, OCT4 and SOX2 expression were analyzed using qRT-PCR. A 2.5-fold activation was obtained after pCXLE-dCas9VP192-T2A-GFP-shP53 with sgOCT4 and sgSOX2 magnetofection in HFF cells compared to the plasmid alone (Figure 7).
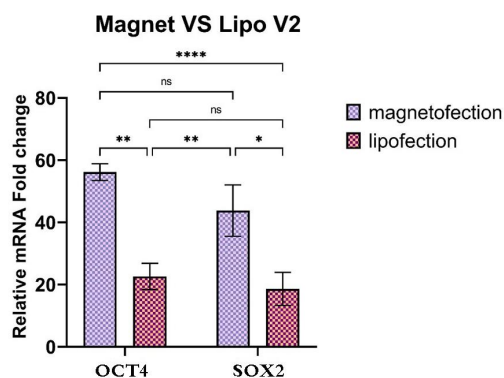

Figure 7. Activation of OCT4 and SOX2 promoters. HFF cells transfected with dCas9VP192 and sgOCT4 and sgSOX2 were analyzed using qRT-PCR 2 days later. dCas9VP192 (control). The asterisks indicate a significant difference (*—$p < 0.05$, **—$p < 0.01$, ****—$p < 0.0001$), ns: non-significant.

4. Discussion

The CRISPR-Cas9 system is a powerful tool that has revolutionized genome engineering in eukaryotic cells and living organisms. Despite the advantage of viral gene delivery, it suffers from low efficacy due in part to unstable DNA/vector complexes in blood circulation and extracellular fluids. However, the surface modification of nanoparticles with PEI enables them to escape from endosomes or prevents the formation of endo-lysosome as a result of the proton sponge effect [21,22]. In this study, we prepared SPIONs coated with PEI [13] to enhance the delivery of CRISPR/Cas9 constructs into human foreskin fibroblast cells. The surface modification of MNPs was performed by conjugating PEI, which enters cargo into a target cell through clathrin-dependent endocytosis, in which positively charged NH2 groups to the negatively charged heparin sulfate proteoglycans on the cells' surfaces [23,24].

According to the results in Figure 2A, the MNPs' diameter had been increased following the formation of PEI-MNPs, which is in line with research conducted by Wang et al. in 2009 [25]. This increase in size might be explained by the presence of PEI, which contained more hydrophilic groups to induce interaction with water molecules. Moreover, the addition of CRISPR/Cas9 plasmid resulted in an increased particle size, which indicates that the presence of DNA and PEI enhanced the particle size. These results are in agreement with published data by Rohiwal et al., showing larger hydrodynamic diameters when a CRISPR/Cas9 plasmid was added to PEI-MNPs in water [4].

As illustrated in Figure 2B, the Zeta potential values of MNPs, PEI-MNPs, and CRISPR/Cas9-PEI-MNPs in the presence of water were found to be positively charged. This result may be correlated to the presence of PEI on the outer layer of MNPs. Moreover, the result showed that the Zeta potential values of all MNP configurations in the presence of DMEM supplemented with 10% FBS became negative. This could be attributed to the adsorption of serum components onto the surface of the complex. A previous study has indicated the colloidal stability of the attachment of the positively charged PEI-CRISPR/Cas9 plasmid complexed in water [4].

As mentioned in Figure 5, a significant improvement in the transfection efficacy was observed after magnetofection compared to lipofection in HFF cells. In a previous study, Steitz and colleagues evaluated the transfection efficiency of superparamagnetic iron oxide nanoparticles coated with PEI (PEI–SPIONs) magnetoplexes with a GFP expressing vector in the COS cells. These showed an enhanced transfection of PEI–SPIONs in a magnetic field [26]. This may be explained by the fact that the magnetic field assists the accumulation of magnetoplexes in the proximity of the cells during transfection, which improves the delivery efficiency [27,28]. On the other hand, the electrical potential represented by a magnetic field can increase the accumulation and the concentrations of the magnetoplexes on the target cell surface. Furthermore, Namgung et al. investigated the application of PEI–SPION magnetoplexes for the gene transfection of HEK-293 cells. They reported that the high transfection ability of CRISPR/Cas9-PEI–SPION in HEK-293 cells was associated with the efficient sedimentation of the magnetoplexes on the HEK-293 cells [28]. Similarly, Hryhorowicz et al. utilized the CRISPR/Cas9-PEI–Mag2 magnetoplexes in the presence of a magnetic field and observed an improvement in transfection efficacy [8]. Our results proved that magnetofection has successfully increased the penetration and subsequent dissociation of the CRISPR/Cas9- PEI-MNP magnetoplexes into the nucleus. Moreover, magnetofection could deliver genes of interest better than lipofectamine 3000.

Furthermore, as illustrated in Figure 6, the cytocompatibility of the magnetoplex was investigated using MTT assay and exhibited a slight reduction in the viability of magnetofected cells, which could be due to the presence of PEI as a proton sponge effect after uptake by the cells, thereby disrupting the endosome/lysosome [29]. A similar outcome was reported by Bajaj et al., who reported that the transfection efficiency and cytocompatibility of PEI–cholesterol-based lipopolymers is associated with the MW of PEI, in which PEI-25kDa was more toxic than other molecular weights of PEI, including 800, 1200, and 2000 kDa [30]. Therefore, another possible reason for the slight increase in cytotoxicity

might be the application of commercially available PEI-25kDa. Similar research was performed by Sadeghi et al., who have evaluated the effect of a superparamagnetic iron oxide coated with poly (ethylene glycol)-grafted PEI (mPEG-co-PEI) on transfection efficiency and cytotoxicity. They reported that the MNP complex displayed a cytotoxicity effect on the NT2 cell line when it was used up to 100 μg/mL for in vitro transfection [31]. In contrast to a previous study, Arsianti et al. reported that the transfection of baby hamster kidney cells (BHK2I) with DNA/PEI + MNP, PEI/MNP + DNA/PEI, or PEI/MNP + DNA + PEI vectors led to significant metabolic activity from 97% to 60% [32].

The data obtained in qRT-PCR in the present study showed a 2.5-fold activation after pCXLE-dCas9VP192-T2A-GFP-shP53 with sgOCT4 and sgSOX2 magnetofection in HFF cells. Our results confirmed that pCXLE-dCas9VP192-T2A-GFP-shP53/sgOCT4 and sgSOX2 magnetoplexes attached to the OCT4 and SOX2 promoters and induced the expression of OCT4 and SOX2 (Figure 7). On the other hand, by using CRISPRa, the robust activation of the endogenous OCT4 and sgSOX2 promoters could be found in both HEK-293 and HFF cells, in which the activation domain VP192 fused with dCas9 could activate the endogenous promoter via two sgRNAs binding to the -150, -630, -260, and -550 bp (sgRNA1 OCT4, sgRNA2 OCT4, sgRNA1 SOX2 and sgRNA2 SOX2, respectively) regions upstream of TSS. A similar study by Cheng et al. described a CRISPRa system, in which one dCas9 activator fused with a VP160 active domain with multiple sgRNAs, enabling binding to the 300 bp region upstream of TSS and allowing efficient gene activation of OCT4, IL1RN, and SOX2 [28]. Another study was published by Lee et al., who quantitatively analyzed using qRT-PCR and found that the activated expression of one of the OSKM genes was up to three-fold higher than that of the other genes, which allowed for the exact control of the cell differentiation [33].

Finally, with the efficiency of the gene delivery system, dCas9-fused VP192 displayed the activation of an endogenous promoter of OCT4 and SOX2 in HFF cells. Further studies are needed to apply PEI-MNPs magnetoplexes to other pluripotency transcription factors in HFF cells and to achieve further optimization for in vivo conditions. This field is open to further future research.

In conclusion, the CRISPR/Cas9 system has emerged as a promising tool for the genome editing of genetic disorders and infectious diseases. The use of a CRISPR/Cas9-PEI-MNP complex with the presence of a magnetic field has been demonstrated to be an effective and nontoxic alternative approach. In this study, we showed that the CRISPR/Cas9-PEI-MNP complex is able to deliver plasmids encoding pCXLE-dCas9VP192-T2A-GFP-shP53 and sgOCT4 and sgSOX2 in HFF cells, enabling the promoter activation of endogenous OCT4 and SOX2. The application of CRISPR/Cas9-PEI-MNPs in combination with a magnetic field was confirmed to be an effective and rapid strategy to develop CRISPR activation. Thus, the local magnetic activation of genome editing and the efficacy of PEI-MNPs for the delivery of a CRISPR/Cas9 genome-editing system for in vivo conditions require future research.

Informed Consent Statement: Informed consent was obtained from all subjects involved in the study.

Data Availability Statement: There is not any raw data (Protein sequences, DNA and RNA sequences, etc.) in this study. All data generated or analyzed are included in the present article.

Conflicts of Interest: The authors declare no competing interests. All authors have participated in conception and design, or analysis and interpretation of the data; drafting the article or revising it critically for important intellectual content; and approval of the final version. This manuscript has not been submitted to, nor is under review at, another journal or other publishing venue. The authors have no affiliation with any organization with a direct or indirect financial interest in the subject matter discussed in the manuscript.

References

1. Cheng, A.W.; Wang, H.; Yang, H.; Shi, L.; Katz, Y.; Theunissen, T.W.; Rangarajan, S.; Shivalila, C.S.; Dadon, D.B.; Jaenisch, R. Multiplexed activation of endogenous genes by CRISPR-on, an RNA-guided transcriptional activator system. *Cell Res.* **2013**, *23*, 1163–1171. [CrossRef] [PubMed]
2. Sun, S.; White, R.R.; Fischer, K.E.; Zhang, Z.; Austad, S.N.; Vijg, J. Inducible aging in Hydra oligactis implicates sexual reproduction, loss of stem cells, and genome maintenance as major pathways. *GeroScience* **2020**, *42*, 1119–1132. [CrossRef] [PubMed]
3. Soufi, A.; Donahue, G.; Zaret, K.S. Facilitators and impediments of the pluripotency reprogramming factors' initial engagement with the genome. *Cell* **2012**, *151*, 994–1004. [CrossRef] [PubMed]
4. Rohiwal, S.; Dvorakova, N.; Klima, J.; Vaskovicova, M.; Senigl, F.; Slouf, M.; Pavlova, E.; Stepanek, P.; Babuka, D.; Benes, H. Polyethylenimine based magnetic nanoparticles mediated non-viral CRISPR/Cas9 system for genome editing. *Sci. Rep.* **2020**, *10*, 4619. [CrossRef] [PubMed]
5. Balboa, D.; Weltner, J.; Eurola, S.; Trokovic, R.; Wartiovaara, K.; Otonkoski, T. Conditionally stabilized dCas9 activator for controlling gene expression in human cell reprogramming and differentiation. *Stem Cell Rep.* **2015**, *5*, 448–459. [CrossRef]
6. Jinek, M. A Programmable Dual-Siswanto, FM, BH Kartiko/Media Sains 1 (2)(2017) 56 J. Media Sains–September 2017 RNA-Guided DNA Endonuclease in Adaptive Bacterial Immunity. *Science* **2012**, *337*, 816–821. [CrossRef]
7. Weltner, J.; Balboa, D.; Katayama, S.; Bespalov, M.; Krjutškov, K.; Jouhilahti, E.-M.; Trokovic, R.; Kere, J.; Otonkoski, T. Human pluripotent reprogramming with CRISPR activators. *Nat. Commun.* **2018**, *9*, 2643. [CrossRef]
8. Hryhorowicz, M.; Grześkowiak, B.; Mazurkiewicz, N.; Śledziński, P.; Lipiński, D.; Słomski, R. Improved delivery of CRISPR/Cas9 system using magnetic nanoparticles into porcine fibroblast. *Mol. Biotechnol.* **2019**, *61*, 173–180. [CrossRef]
9. Glass, Z.; Lee, M.; Li, Y.; Xu, Q. Engineering the delivery system for CRISPR-based genome editing. *Trends Biotechnol.* **2018**, *36*, 173–185. [CrossRef]
10. Rajendrakumar, S.K.; Uthaman, S.; Cho, C.S.; Park, I.-K. Trigger-responsive gene transporters for anticancer therapy. *Nanomaterials* **2017**, *7*, 120. [CrossRef]
11. Prijic, S.; Sersa, G. Magnetic nanoparticles as targeted delivery systems in oncology. *Radiol. Oncol.* **2011**, *45*, 1–16. [CrossRef] [PubMed]
12. Huang, S.-J.; Ke, J.-H.; Chen, G.-J.; Wang, L.-F. One-pot synthesis of PDMAEMA-bound iron oxide nanoparticles for magnetofection. *J. Mater. Chem. B* **2013**, *1*, 5916–5924. [CrossRef] [PubMed]
13. Li, N.; Liu, T.; Chen, H.; Liao, J.; Li, H.; Luo, Q.; Song, H.; Xiang, F.; Tan, J.; Zhou, J. Management strategies for the burn ward during COVID-19 pandemic. *Burns* **2020**, *46*, 756–761. [CrossRef]
14. Bi, Q.; Song, X.; Hu, A.; Luo, T.; Jin, R.; Ai, H.; Nie, Y. Magnetofection: Magic magnetic nanoparticles for efficient gene delivery. *Chin. Chem. Lett.* **2020**, *31*, 3041–3046. [CrossRef]
15. Lo, Y.-L.; Chou, H.-L.; Liao, Z.-X.; Huang, S.-J.; Ke, J.-H.; Liu, Y.-S.; Chiu, C.-C.; Wang, L.-F. Chondroitin sulfate-polyethylenimine copolymer-coated superparamagnetic iron oxide nanoparticles as an efficient magneto-gene carrier for microRNA-encoding plasmid DNA delivery. *Nanoscale* **2015**, *7*, 8554–8565. [CrossRef]
16. Grześkowiak, B.F.; Hryhorowicz, M.; Tuśnio, K.; Grzeszkowiak, M.; Załęski, K.; Lipiński, D.; Zeyland, J.; Mykhaylyk, O.; Słomski, R.; Jurga, S. Generation of transgenic porcine fibroblast cell lines using nanomagnetic gene delivery vectors. *Mol. Biotechnol.* **2016**, *58*, 351–361. [CrossRef]
17. Kim, J.B.; Sebastiano, V.; Wu, G.; Araúzo-Bravo, M.J.; Sasse, P.; Gentile, L.; Ko, K.; Ruau, D.; Ehrich, M.; van den Boom, D.; et al. Oct4-induced pluripotency in adult neural stem cells. *Cell* **2009**, *136*, 411–419. [CrossRef]
18. Tiwari, A.P.; Rohiwal, S.S.; Suryavanshi, M.V.; Ghosh, S.J.; Pawar, S.H. Detection of the genomic DNA of pathogenic α-proteobacterium Ochrobactrum anthropi via magnetic DNA enrichment using pH responsive BSA@ Fe$_3$O$_4$ nanoparticles prior to in-situ PCR and electrophoretic separation. *Microchim. Acta* **2016**, *183*, 675–681. [CrossRef]

19. Wightman, L.; Kircheis, R.; Rössler, V.; Carotta, S.; Ruzicka, R.; Kursa, M.; Wagner, E. Different behavior of branched and linear polyethylenimine for gene delivery in vitro and in vivo. *J. Gene Med. Cross-Discip. J. Res. Sci. Gene Transf. Clin. Appl.* **2001**, *3*, 362–372.

20. Zhang, L.; Li, Y.; Jimmy, C.Y.; Chen, Y.Y.; Chan, K.M. Assembly of polyethylenimine-functionalized iron oxide nanoparticles as agents for DNA transfection with magnetofection technique. *J. Mater. Chem. B* **2014**, *2*, 7936–7944. [CrossRef]

21. Freeman, E.C.; Weiland, L.M.; Meng, W.S. Modeling the proton sponge hypothesis: Examining proton sponge effectiveness for enhancing intracellular gene delivery through multiscale modeling. *J. Biomater. Sci. Polym. Ed.* **2013**, *24*, 398–416. [CrossRef]

22. Ma, Y.; Zhang, Z.; Wang, X.; Xia, W.; Gu, H. Insights into the mechanism of magnetofection using MNPs-PEI/pDNA/free PEI magnetofectins. *Int. J. Pharm.* **2011**, *419*, 247–254. [CrossRef] [PubMed]

23. Pichon, C.; Gonçalves, C.; Midoux, P. Histidine-rich peptides and polymers for nucleic acids delivery. *Adv. Drug Deliv. Rev.* **2001**, *53*, 75–94. [CrossRef] [PubMed]

24. Ota, S.; Takahashi, Y.; Tomitaka, A.; Yamada, T.; Kami, D.; Watanabe, M.; Takemura, Y. Transfection efficiency influenced by aggregation of DNA/polyethylenimine max/magnetic nanoparticle complexes. *J. Nanoparticle Res.* **2013**, *15*, 1653. [CrossRef]

25. Wang, X.; Zhou, L.; Ma, Y.; Li, X.; Gu, H. Control of aggregate size of polyethyleneimine-coated magnetic nanoparticles for magnetofection. *Nano Res.* **2009**, *2*, 365–372. [CrossRef]

26. Steitz, B.; Hofmann, H.; Kamau, S.W.; Hassa, P.O.; Hottiger, M.O.; von Rechenberg, B.; Hofmann-Amtenbrink, M.; Petri-Fink, A. Characterization of PEI-coated superparamagnetic iron oxide nanoparticles for transfection: Size distribution, colloidal properties and DNA interaction. *J. Magn. Magn. Mater.* **2007**, *311*, 300–305. [CrossRef]

27. Li, L.; Hu, S.; Chen, X. Non-viral delivery systems for CRISPR/Cas9-based genome editing: Challenges and opportunities. *Biomaterials* **2018**, *171*, 207–218. [CrossRef]

28. Namgung, R.; Singha, K.; Yu, M.K.; Jon, S.; Kim, Y.S.; Ahn, Y.; Park, I.-K.; Kim, W.J. Hybrid superparamagnetic iron oxide nanoparticle-branched polyethylenimine magnetoplexes for gene transfection of vascular endothelial cells. *Biomaterials* **2010**, *31*, 4204–4213. [CrossRef]

29. Tomitaka, A.; Koshi, T.; Hatsugai, S.; Yamada, T.; Takemura, Y. Magnetic characterization of surface-coated magnetic nanoparticles for biomedical application. *J. Magn. Magn. Mater.* **2011**, *323*, 1398–1403. [CrossRef]

30. Bajaj, A.; Kondaiah, P.; Bhattacharya, S. Synthesis and gene transfection efficacies of PEI− cholesterol-based lipopolymers. *Bioconjugate Chem.* **2008**, *19*, 1640–1651. [CrossRef]

31. Sadeghi, Z.; Maleki, P.; Shahabi, F.; Bondarkhilli, S.A.M.; Masoumi, M.; Taheri, M.; Mohammadi, M.; Raheb, J. Surface modification of superparamagnetic iron oxide (SPION) and comparison of cytotoxicity effect of mPEG2000-PEI-SPION and mPEG750-PEI-SPION on the human embryonic carcinoma stem cell, NTERA2 cell line. *Hum. Antibodies* **2020**, *28*, 159–167. [CrossRef]

32. Arsianti, M.; Lim, M.; Marquis, C.P.; Amal, R. Assembly of polyethylenimine-based magnetic iron oxide vectors: Insights into gene delivery. *Langmuir* **2010**, *26*, 7314–7326. [CrossRef]

33. Lee, M.H.; Lin, C.C.; Thomas, J.L.; Li, J.A.; Lin, H.Y. Cellular reprogramming with multigene activation by the delivery of CRISPR/dCas9 ribonucleoproteins via magnetic peptide-imprinted chitosan nanoparticles. *Mater. Today Bio* **2021**, *9*, 100091. [CrossRef]